IOP Publishing Journal of Physics B: Atomic, Molecular and Optical Physics
J. Phys. B: At. Mol. Opt. Phys. **49** (2016) 035701 (9pp) doi:10.1088/0953-4075/49/3/035701

Dynamic Stark broadening of Lyman-α

Evgeny Stambulchik[1] **and Alexander V Demura**[2]

[1] Faculty of Physics, Weizmann Institute of Science, Rehovot 7610001, Israel
[2] National Research Centre 'Kurchatov Institute', Kurchatov Square 1, Moscow 123182, Russian Federation

E-mail: Evgeny.Stambulchik@weizmann.ac.il and Demura_AV@nrcki.ru

Received 8 June 2015, revised 21 October 2015
Accepted for publication 26 October 2015
Published 21 January 2016

Abstract

Calculating lineshapes of atomic radiative transitions broadened by plasma is a complex problem lacking a general analytic solution, and several models have been suggested to treat it. Lyman-α is the simplest transition; paradoxically however, calculating the broadening of this spectral line in plasma results in a significant spread between different models. Here, we argue that the quasistatic broadening regime is never realized for the line core in a one-component plasma; instead, the broadening due to either electrons or ions alone evolves from the impact regime to another regime, also dynamical in nature. In the latter (referred to here as 'rotational' broadening), the linewidth only depends on the typical frequency of the plasma microfields and is independent of both the microfield magnitudes and the atomic properties of the transition. We also demonstrate that rotational broadening is asymptotically reached in the high-density/low-temperature limit by other transitions with an unshifted central component, such as the Balmer-α line. A simple expression is suggested interpolating between the two asymptotic regimes, applicable to broadening due to electrons and ions alike. The treatment is further extended to realistic two-component plasmas. Comparison to results of accurate computer simulations shows a good agreement over a very large range of plasma parameters, both for the case of one- and two-component plasmas.

Keywords: plasma line broadening, ion dynamics, computer simulations

(Some figures may appear in colour only in the online journal)

1. Introduction

The problem of calculating lineshapes of atomic radiative transitions broadened by plasma is of high importance for pure and applied science [1]. However, after more than half a century of development of the quantum theories of plasma Stark broadening [2], a truly unified analytic description of plasma-broadened lineshapes remains elusive. The plasma microfield dynamics is characterized by extremely wide ranges of field magnitudes and frequencies, due to the practically infinite spread of particle velocities and inter-particle distances realized in the course of thermal motion of the plasma particles, and is further complicated by collective effects. Evolution of an atomic system in such an external time-dependent electric field $\vec{F}(t)$ cannot, in general, be obtained analytically, and several models have been suggested to address this complex problem [3].

Even for an ideal one-component plasma (OCP), finding the evolution of the simplest realistic atomic model required for obtaining the Lyman-α ($n=2$ to $n'=1$ transition in hydrogen or a hydrogen-like ion) shape remains possible only numerically, or by using various approximations or semi-empirical models. One may wonder why this holds true, despite the ideal OCP magnitude and frequency distributions being analytically derived in the first half of the previous century [4, 5]. A plausible answer is that the magnitude and frequency distributions *taken separately* are insufficient to describe the full dynamics of the plasma fields and, therefore, evolution of the radiator. Indeed, as a result of plasma particle motion, not only does the total field experienced by the radiator change in magnitude, but its direction is varied as well, and these two effects are *not independent* [5, 6]. The different modes of the microfield fluctuations and respective different effects on line broadening were first analyzed based on, and extending, the framework of the 'standard theory'

(ST) of plasma line broadening almost four decades ago [7], and recently became a subject of study again [6, 8], this time beyond a perturbative approach.

Following [6, 8], one introduces 'rotational' and 'vibrational' pseudocomponents of the total microfield $\vec{F}(t)$, defined as

$$\vec{F}_{\rm rot}(t) = F_0 \frac{\vec{F}(t)}{F(t)} \tag{1}$$

and

$$\vec{F}_{\rm vib}(t) = \vec{n} F(t), \tag{2}$$

respectively, where $\vec{n}$ is a unity vector aligned, for example, along the z-axis. It was shown [6] that the central part of the Lyman-α Stark profile is largely determined by the 'rotational' perturbation. Furthermore, for the range of plasma parameters considered, the linewidth appeared to scale as $\propto v_i N_i^{1/3}$, where N_i and v_i are the ion density and thermal velocity, respectively. In other words, broadening depends on the typical field fluctuation rate, but not on its magnitude.

In the present study, we show that this is a general result in the OCP high-density/low-temperature limit, and construct a unified expression that covers a broad range of plasma parameters, and applies, unmodified, to both electrons and any type of ions. Furthermore, we demonstrate applicability of this model to the case of line broadening by realistic two-component plasmas (TCPs).

The paper is organized as follows. The first part is limited in scope to line broadening by an ideal OCP. In section 2.1 we show, by invoking straightforward dimensionality considerations, that the width of an atomic transition with a linear Stark effect *may*, in general, have the 'rotational' type of scaling and that, furthermore, it *must* be realized if the width is dominated by the broadening of the central Stark component. We prove this by extensive computer simulations of Lyman-α Stark broadening presented in section 2.2 and introduce a semi-empiric expression interpolating between the rotational and impact asymptotic dependences. In section 2.3 we demonstrate applicability of these findings to other lines with an unshifted central component.

In section 3.1 we turn our attention to Stark broadening by a TCP, ignoring interactions between the plasma particles. We show that the simple model derived for the OCP can be easily extended for the TCP case and, again, prove the validity by comparison with computer simulations over a wide range of plasma parameters. Section 3.2 concludes the second part of the study by discussing corrections to account for plasma non-ideality.

Section 4 is devoted to discussing related issues, considered in the context of the rotational regime of line broadening. Finally, we conclude by summarizing our findings in section 5.

2. Ideal one-component plasma

2.1. Dimensionality analysis

For a transition between atomic states i and j, one can construct three entities with the dimension of energy (or frequency; throughout the text, we use atomic units where $\hbar = 1$): The static Stark effect $w_{\rm st} \equiv \Delta E_i - \Delta E_j$; $w_{\rm dyn}$, which is a typical value of the instantaneous frequency of the electric field

$$\nu = \dot{F}(t)/F(t); \tag{3}$$

and the unperturbed transition energy E_{ij}^0 itself.

Limiting our study to hydrogen-like atomic system and neglecting fine structure and quadratic and higher-order Stark effects, i.e., considering a pure degenerate atomic system, we write

$$w_{\rm st} \sim \left(d_i - d_j\right) F_0 \propto \frac{|Z_p|}{Z} N_p^{2/3}, \tag{4}$$

where $F_0 = 2\pi \left(\frac{4}{15}\right)^{2/3} Z_p N_p^{2/3}$ is the Holtsmark field [4] due to the plasma particles with charge Z_p and density N_p, d_i and d_j are the electric dipole moments of the states i and j, respectively, and Z is the atomic number of the radiator ($Z = 1$ corresponds to hydrogen). This simplified expression further assumes negligible influence of the plasma temperature on the microfield distribution, i.e. the model of a very weakly coupled plasma. Under the same assumption, the 'dynamic' entity is, evidently,

$$w_{\rm dyn} \sim v/r \sim \sqrt{T/M_p^*}\, N_p^{1/3}, \tag{5}$$

where v and r are, respectively, the typical velocity and interparticle distances (relative to the radiator), and $M_p^* = M_p M_r/(M_p + M_r)$ is the perturber reduced mass (in the center-of-mass frame of the radiator and the perturber with the masses M_r and M_p, respectively).

As long as both $w_{\rm st}$ and $w_{\rm dyn}$ remain small compared to E_{ij}^0, the latter can be excluded from the consideration. We further simplify our task of finding the plasma-broadened spectrum by focusing on the most important property of a lineshape, its width w (specifically, the full width at half maximum, FWHM).

From dimensionality considerations, w can be written as

$$w = \sum_k C_k w_{\rm st}^{p_k} w_{\rm dyn}^{1-p_k} \equiv \sum_k C_k w_k, \tag{6}$$

where C_k and p_k are real numbers. w_k is then

$$w_k \propto \left(\frac{|Z_p|}{Z}\right)^{p_k} \left(\frac{T}{M_p^*}\right)^{(1-p_k)/2} N_p^{(1+p_k)/3}. \tag{7}$$

It is interesting to analyze some specific values of p_k, focusing in particular on the N_p and T dependences. For example, $p_k = 1$ corresponds to the quasistatic limit [9, 10] of line broadening, with $w_k \sim w_{\rm st} \propto N_p^{2/3}$ (neglecting Debye screening corrections and other particle correlation effects). $p_k = 2$ corresponds to another well known limit, the impact

approximation [9], with the leading (up to the logarithmic terms) $w_k \propto N_p/\sqrt{T}$ dependence.

It appears that plasma spectral line broadening 'common wisdom', replicated in numerous studies, assumes these two limiting cases (the quasistatic and impact broadening mechanisms) as being asymptotically approached by any transition in the low-T/high-N_p and high-T/low-N_p limits, respectively.

Here, we argue that this is not always the case. Indeed, if $w_{\rm st} \ll w_{\rm dyn}$, or even when $w_{\rm st}$ is exactly zero, the only non-vanishing term in the sum given in equation (6) is that with $p_k = 0$. Then unavoidably, $w \propto w_{\rm dyn}$, i.e. line broadening becomes *independent* of the plasma field magnitude, being only proportional to its (typical) fluctuation rate. An obvious way to solve this apparently paradoxical conclusion is to put the corresponding $C_k \equiv 0$, which would indeed be correct for a transition with a *single* unshifted component. However, the question is then raised for the case where only part of the components have zero static Stark shift, while the others have finite shifts. This is indeed the case for hydrogen-like transitions between levels where the principal quantum numbers differ by an odd number (see, for example, [11]), in particular, the Lyman-α line. We show that in such a case, the correct low-T/high-N_p asymptotic dependence is indeed $w \sim w_{\rm dyn} \propto \sqrt{T}N_p^{1/3}$ (which we call the 'rotational' approximation) and not the quasistatic $\propto N_p^{2/3}$ one. Furthermore, we claim that for such lines (with an unshifted central component) the quasistatic $\propto N_p^{2/3}$ dependence is only approximately realized as an intermediate case in transition between the impact and rotational broadening regimes.

2.2. Lyman-α broadening by an ideal one-component plasma

Computer simulations (CSs) of spectral line broadening are often considered as *ab initio* calculations and their results regarded as benchmarks—at least for hydrogen-like transitions [12]. Furthermore, CSs provide a unique possibility to model idealized conditions that cannot be realized experimentally, such as an OCP or a plasma consisting of fractional-charge particles. The CS calculations consist of two parts: simulating the motion of plasma particles, resulting in sufficiently complete microfield histories; and solving the radiator evolution problem by using the field histories as a time-dependent perturbation. We use a specific implementation of CS lineshape calculations described in [13].

We consider hydrogen Lyman-α broadened by an OCP consisting of protons ($Z_p = 1$ and $M_p^* = m_p/2$, where m_p is the proton mass). In order to filter out corrections due to collective plasma effects (e.g. Debye shielding), we neglect interactions between protons. We further assume the non-quenching approximation, i.e. neglect spin–orbital coupling, mixing of states with different principal quantum numbers, and other than dipole interactions between the perturber particles and the radiator. Our 'reference' plasma conditions are $T = 1\,{\rm eV}$ and $N_p = 10^{17}{\rm cm}^{-3}$. 8000 particles were included in the simulations.

Within the ideal OCP model, any variation in T, Z_p, N_p and M_p from their respective reference values is reduced to only two multiplicative factors, the field strength scale s_F and the time dilation scale s_t,

$$s_F = \left|\frac{Z_p}{Z_p^0}\right|\left(\frac{N_p}{N_p^0}\right)^{2/3} \tag{8}$$

and

$$s_t = \left(\frac{N_p^0}{N_p}\right)^{1/3}\left(\frac{T^0 M_p^*}{T M_p^{0*}}\right)^{1/2}. \tag{9}$$

Thus, a given set of microfield histories can be reused to model an infinite number of plasma conditions. In addition to reducing the computational effort, we avoid numerical uncertainties due to statistical 'noise' which are inherent to CS methods, since for each set of plasma parameters the field histories used are statistically equivalent.

We start by varying the perturber charge Z_p. As described above, this is achieved by multiplying the field magnitudes by Z_p ($s_F = Z_p$). By varying Z_p, and hence $w_{\rm st}$ (see equation (4)) by three orders of magnitude, we cover cases where $w_{\rm st} \ll w_{\rm dyn}$ and $w_{\rm st} \gg w_{\rm dyn}$, as well as intermediate cases. (Although, contrary to the particle mass, temperature and number density, particle charge in reality may assume only integer values, treating it as a continuous entity—including fractional values less than unity—is a convenient way to analyze various scaling relations.) Lineshapes for a few values of Z_p are shown in figure 1. In the reference case of $Z_p = 1$ one can see that the central component partially overlaps with the lateral components (the spectra are symmetric within the approximations assumed, and hence the 'red' parts of the spectra are not shown). With the smaller $Z_p = 1/4$, we move toward the impact regime ($w_{\rm dyn} \gg w_{\rm st}$), and the lineshape largely loses any discernible structure, approaching a Lorentzian shape. Increasing Z_p to 4 separates the central and lateral components by broadening and pushing the lateral components away from the origin (proportional to Z_p) while the width of the central component remains *largely constant*. Evidently, when the lateral components are progressively shifted and broadened (as seen in the semi-

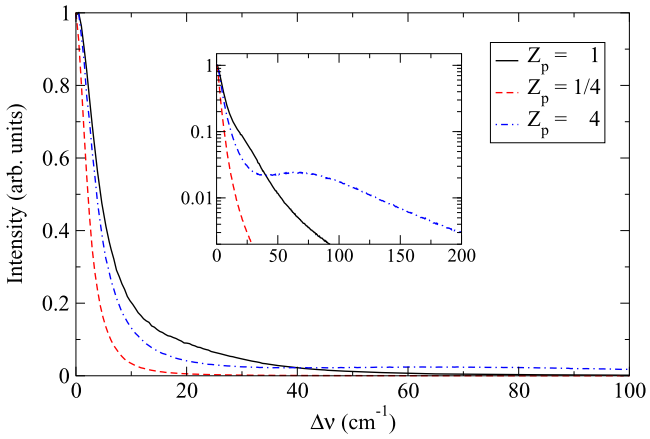

Figure 1. Peak-normalized CS half-profiles of Lyman-α in an ideal OCP with $T = 1$ eV and $N_p = 10^{17}$ cm^{-3}, assuming different values of Z_p.

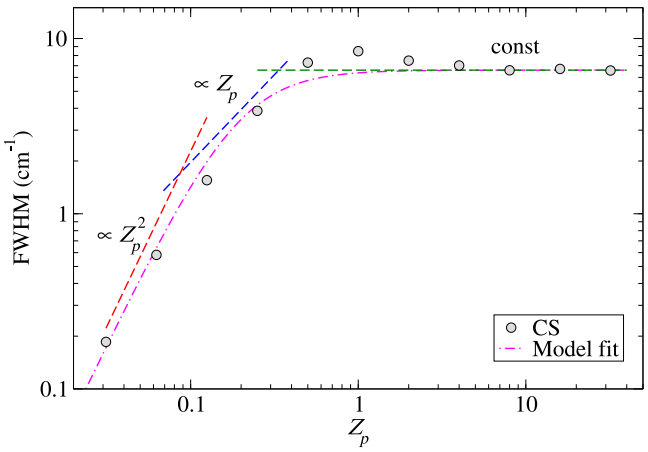

Figure 2. FWHM of Lyman-α in an ideal OCP with $T = 1$ eV and $N_p = 10^{17}$ cm^{-3} as a function of Z_p. CS results are shown as well as functional asymptotic dependences of different approximations. Also shown is a model fit according to equation (14).

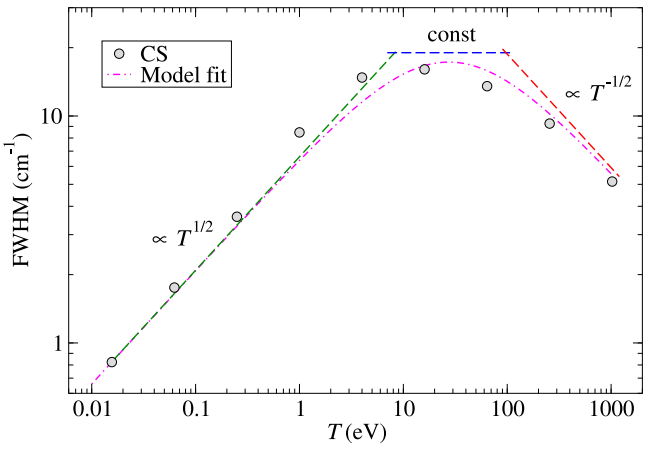

Figure 3. Same as figure 2, but keeping $Z_p = 1$ constant and varying T instead.

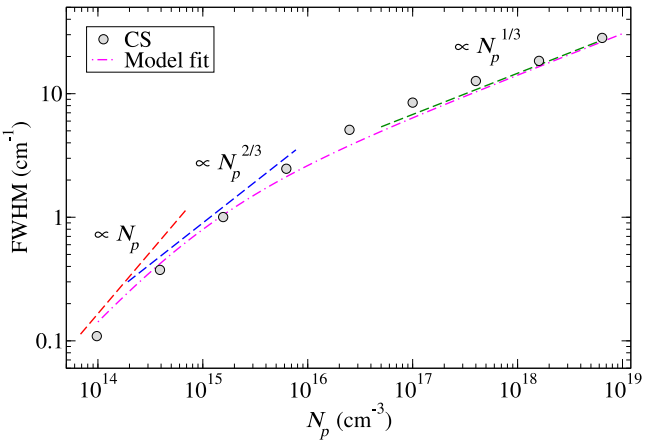

Figure 4. Same as figure 2, but varying N_p instead.

logarithmic scale in the inset of the figure), while the central component is not, the line FWHM becomes mainly determined by the width of the central component.

The results are shown in figure 2. In the $Z_p \to 0$ limit, the linewidth has a $\propto Z_p^2$ dependence, corresponding to the impact approximation, see equation (7), as anticipated. However, in the opposite $Z_p \to \infty$ limit, the width approaches a constant *finite* value, contrary to the ST-based expectation.

What does this constant value depend on? Based on our qualitative dimensionality arguments, it should be proportional to $w_{\rm dyn}$, i.e. $\propto\sqrt{T}$ if N_p is kept constant. To verify this, we calculated a series of Lyman-α profiles by varying T. Similar to what was done for varying Z_p, the same microfield histories were reused, but the values of the time step were changed as $\propto 1/\sqrt{T}$. The results are presented in figure 3. We note that our 'reference' plasma with $T = 1$ eV is at the onset of the Z_p-independent regime (see figure 2). Therefore, by decreasing T we are guaranteed to remain in this regime. Indeed, varying T by two orders of magnitude towards lower values, down to 0.01 eV, one observes that the linewidth scales proportionally to $\sqrt{T}$ as long as $w_{\rm st} \gg w_{\rm dyn}$, therefore firmly confirming our expectation. Varying T in the opposite direction, the linewidth growth slows down and at some further point line broadening begins to decrease, eventually approaching the impact-limit T dependence $\propto 1/\sqrt{T}$. Evidently, the microfield dynamics is not influenced by temperature alone, but by the perturber velocities $\sim\sqrt{T/M_p^*}$. Therefore, the same effect is observed when scaling the reduced perturber mass M_p^*.

Finally, we investigate the N_p dependence. Here (see figure 4), the Lyman-α linewidth scales as $\propto N_p^{1/3}$ as well at high densities and slowly approaches the $\propto N_p$ impact asymptote toward lower values of N_p.

Thus, we have numerically confirmed the existence of a *new* regime of plasma line broadening, in which the linewidth depends on N_p, T and M_p^* as $w \propto N_p^{1/3}(T/M_p^*)^{1/2}$, and is entirely independent of Z_p. This is radically different from both the impact ($w \propto Z_p^2 N_p (T/M_p^*)^{-1/2}$) and quasistatic ($w \propto |Z_p| N_p^{2/3}$) approximations.

It is important to note that the quasistatic regime, strictly speaking, is *never* realized for a spectral line with an unshifted Stark component, such as Lyman-α, but only as a transitional case between the two true asymptotic regimes, i.e. the impact and the rotational broadenings. This is clearly seen from figures 2–4. The 'critical' values (corresponding to transition between the asymptotic regimes) of the plasma parameters and their functional dependences on the other ones are readily obtained by requiring equivalence of the characteristic static (equation (4)) and dynamic (equation (5)) Stark effect entities. For example,

$$Z_p^{(\rm cr)} \propto Z\left(T/M_p^*\right)^{1/2} N_p^{-1/3}, \tag{10}$$

$$T^{(\rm cr)} \propto M_p^* \left(Z_p/Z\right)^2 N_p^{2/3}, \tag{11}$$

and

$$N_p^{(\rm cr)} \propto \left(Z/|Z_p|\right)^3 \left(T/M_p^*\right)^{3/2}. \tag{12}$$

It is possible to construct a general semi-empiric analytic expressions for the Lyman-α width w approximating over a broad plasma parameter range. In the simplest form, it can be

written as

$$w^{-1} = w_{\rm imp}^{-1} + w_{\rm rot}^{-1}, \tag{13}$$

where $w_{\rm imp}$ and $w_{\rm rot}$ are the Stark broadenings in the impact and rotational limits, respectively. Recalling that the impact and rotational regimes correspond, respectively, to $p_k = 2$ and 0 in equation (7), we obtain

$$w^{-1} = \alpha \left(\frac{Z}{Z_p}\right)^2 \left(\frac{T}{M_p^*}\right)^{1/2} N_p^{-1} + \beta^{-1} \left(\frac{M_p^*}{T}\right)^{1/2} N_p^{-1/3}, \tag{14}$$

where α and β are some constants. Best-fit curves corresponding to this model are displayed in figures 2–4. By construction (see equation (13)), these curves should match the true FWHM values in the $\to 0$ and $\to \infty$ limits of a plasma parameter being varied, since only one—either the impact or rotational regime—is fully dominant in each of these limits. However, even in the intermediate regimes, deviations of this simple model from the accurate calculation results are within 10–20%.

2.3. Other lines with unshifted central component

Although the focus of the present study is on Lyman-α, it is instructive to also analyze other hydrogen-like transitions with a central component. Let us choose specific proportionality coefficients for $w_{\rm dyn}$ and $w_{\rm st}$ in equations (4) and (5), respectively. For consistency with a previous study [14], we use

$$w_{\rm dyn} = \sqrt{\frac{T}{M_p^*}} \left(\frac{4\pi}{3} N_p\right)^{1/3}, \tag{15}$$

and define

$$w_{\rm qs} = 6\pi\,(4/15)^{2/3} \bar{\omega}_{1/2}^0 \frac{|Z_p|}{Z} \left(n^2 - n'^2\right) N_p^{2/3} \tag{16}$$

as an effective quasistatic broadening of a multi-component line in the quasicontiguous (QC) approximation [14]. Here, $\bar{\omega}_{1/2}^0 \approx 1.44$.

With these definitions, expression (14) can conveniently be rewritten as

$$w = w_{\rm qs} \left(\frac{\bar{\alpha}}{R} + \frac{R}{\bar{\beta}}\right)^{-1} \equiv w_{\rm dyn} \left(\frac{\bar{\alpha}}{R^2} + 1/\bar{\beta}\right)^{-1}, \tag{17}$$

where R is a ratio between $w_{\rm qs}$ and $w_{\rm dyn}$,

$$R = w_{\rm qs}/w_{\rm dyn} \approx 7 \frac{|Z_p| \left(n^2 - n'^2\right) M_p^{*1/2} N_p^{1/3}}{Z T^{1/2}} \tag{18}$$

(we remind the reader that atomic units are used over the entire discussion). In the notation provided by equation (17), both $\bar{\alpha}$ and $\bar{\beta}$ become dimensionless. Furthermore, since the atomic properties are absorbed in R and $w_{\rm dyn}$ depends only on the plasma 'bath' dynamics, the second form of equation (17) should represent a universal dependence of line broadening on R as long as the model assumed (equation (13)) remains physically sound. Based on the best-fit model curves shown in figures 2–4, $\bar{\alpha}$ and $\bar{\beta}$ were determined to be approximately equal to 2 and 1.2, respectively.

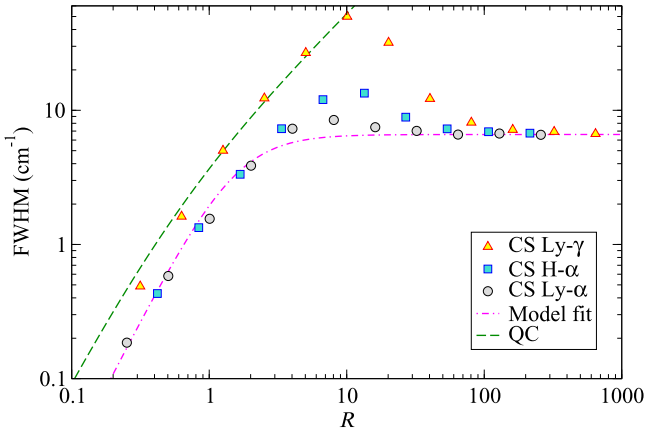

Figure 5. FWHM of Lyman-α, Balmer-α and Lyman-γ in an ideal OCP with $T = 1$ eV and $N_p = 10^{17}$ cm^{-3} (corresponding to $w_{\rm dyn} \approx 5.50$ cm^{-1}) as a function of R (equation (18)). CS results are shown as well as a model fit according to equation (17) with $\bar{\alpha} = 2$ and $\bar{\beta} = 1.2$. It is seen that in the rotational regime ($R \gg 1$), the widths of all lines asymptotically approach the same value. Also shown is the QC approximation (equation (19)), labelled 'QC'.

Figure 5 is equivalent to figure 2 with the abscissas expressed in units of R. In addition to the FWHM of Lyman-α, we also plot FWHMs of hydrogen Balmer-α ($n = 3$ to $n' = 2$) and Lyman-γ ($n = 4$ to $n' = 1$) transitions. Most notably, in the 'rotational' limit ($R \to \infty$), the widths of *all* lines asymptotically approach the same value, in full accordance with equation (17), predicting it to be $\bar{\beta} w_{\rm dyn} \approx 1.2 w_{\rm dyn}$. In the opposite limit ($R \to 0$) both $\Delta n = 1$ lines, i.e. Lyman-α and Balmer-α, also depend on R identically, approaching the impact broadening regime. On the other hand, in the intermediate regime ($R \sim 10$) the linewidths behave differently, with that of Lyman-α being the closest to the model (equation (17)), and that of Lyman-γ the farthest. This is to be expected, since the weight of the central component (which is strongly affected by the microfield dynamics) relative to the total line intensity is the largest for Lyman-α and the smallest for Lyman-γ, with Balmer-α in between. Therefore, in the intermediate region where the overlap between the central and lateral components is significant, the linewidth is affected by the shapes of the lateral components, and the weaker the central component is, the more pronounced this effect becomes. In the $\Delta n \to \infty$ limit, the relative contribution of the central component becomes zero and the rotational regime is never approached; instead, the impact broadening regime slowly changes to the quasistatic one. This transition should be well described by the QC approximation, derived assuming $\Delta n \gg 1$. In this approximation, line broadening due to an ideal OCP is given [14] as

$$w_{\rm qc} = w_{\rm qs} \left(\frac{R_0}{R} + 1\right)^{-1} \equiv w_{\rm dyn} \left(\frac{R_0}{R^2} + 1/R\right)^{-1}, \tag{19}$$

where $R_0 = 0.5$ is an empiric constant chosen to best fit the transition between the impact and quasistatic regimes. It is seen from figure 5 that even for the relatively small $\Delta n = 3$ of Lyman-γ, the QC model (equation (19)) accurately approximates the broadening of this line up to moderate values of R.

We would like to note that except for the impact limit, where an entire lineshape has a simple Lorentzian shape, the use of a single parameter (in this case, FWHM) to describe a complex lineshape is evidently incomplete and may or may not suffice for specific needs. In particular, the Lyman-α FWHM is largely unaffected by the lateral components. However, if the line is strongly broadened by an additional mechanism, such as the Doppler effect or resonance self-absorption (opacity), the shape and position of the lateral components may become crucial. The lateral components, contrary to the central one, are sensitive to the microfield magnitudes (equation (2)) and therefore attain shapes correctly described by the quasistatic approximation in the $R \to \infty$ limit.

3. Two-component plasmas

3.1. Lyman-α broadening by an ideal two-component plasma

Up to now, we have only considered a one-component proton plasma. However, the model (equation (17)) is also applicable to other types of ions as well as to electrons. Let us now investigate a more realistic TCP consisting of protons and electrons (however, we still assume non-interacting plasma particles). Thus, we calculate contributions to the Lyman-α width due to ions w_i and electrons w_e separately, and then sum them up arithmetically,

$$w_{\rm tot} = w_i + w_e. \tag{20}$$

We stress that for both ions and electrons the $\bar{\alpha}$ and $\bar{\beta}$ constants in equation (17) are *exactly the same*, with the only difference being the reduced perturber mass M_p^* in evaluation of R (equation (18)), $m_p/2$ for protons and $\approx m_e$ for electrons.

Temperature and density dependences of the Lyman-α FWHM in such a TCP are shown in figures 6 and 7, respectively. The total linewidths, as given by the simple model according to equations (17), (18) and (20), are compared to TCP CS results, calculated for a few values of temperature and density. Except for the lowest T point in figure 6 (which will be discussed below), the comparisons demonstrate a very good agreement. It is important to note that while each of the ion and electron contributions varies significantly with T, the total width is almost constant over a temperature range of four orders of magnitude, resulting from coincidental cancellation of the electron and ion T dependences due to the vastly different masses: in the region where electrons and ions contribute comparably, electrons are nearly in the impact regime (their contribution decreases with T) while ions are in the rotational regime (their contribution increases with T), while towards the lower/upper values of T from this central region electrons/ions reach their respective

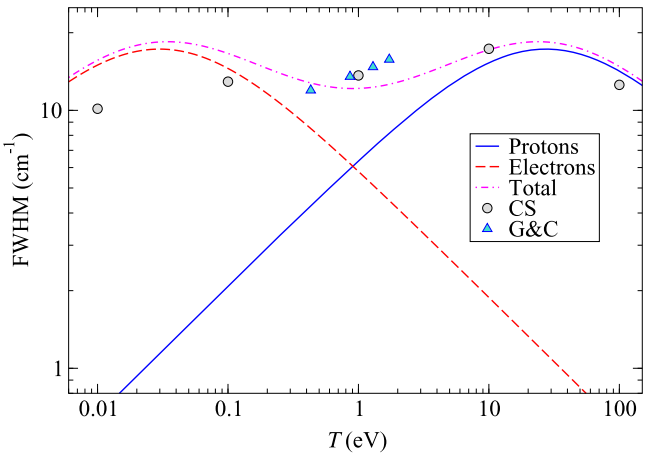

Figure 6. FWHM of Lyman-α in an ideal TCP as a function of T: comparison of CS results with the model. $N_p = 10^{17}$ cm^{-3} is assumed. Also shown are results for *non-ideal* hydrogen TCP from the reference diagnosis tables [15] (labelled here as 'G&C').

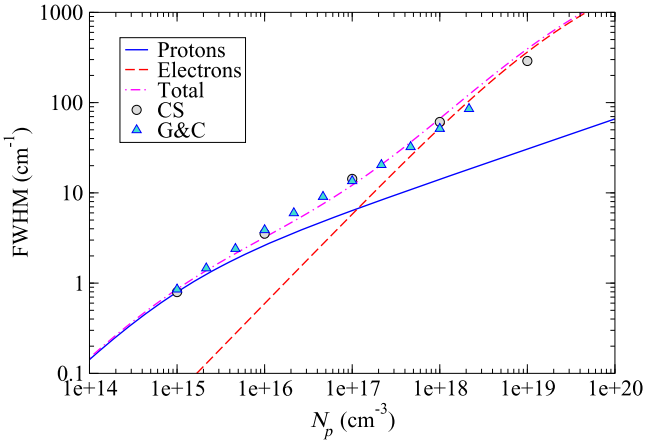

Figure 7. Same as figure 6, but as a function of N_p assuming $T = 1$ eV.

critical $T^{\rm cr}$s (eqauation (11)), where the temperature dependence nearly disappears.

Considering now the density dependence (figure 7), we observe a similar phenomenon: the region of N_p where ions and electrons contribute comparably corresponds to different broadening regimes (rotational and impact, respectively). As a result, the total density dependence over many orders of magnitude is nearly $\propto N_p^{2/3}$, a kind of average between $N_p^{1/3}$ and N_p.

In general, the arithmetic sum (equation (20)) is not a good approach when the two Stark broadening contributions are accounted for. However, as discussed above, the plasma parameter regions when the ion and electron contributions become comparable happen to correspond to nearly rotational/impact regimes, respectively, for both of which the line core profile assumes a Lorentzian shape. Together with the assumption of statistical independence of the two broadening mechanisms, expression (20) becomes almost exact in these regions. In areas of practical interest outside of these regions, only one of the ion or electron broadenings is strongly

dominant, in which case the inaccuracy introduced by this simple approach becomes unimportant.

We note that the *effective* T and N_p dependences of the Lyman-α width in the TCP (nearly constant and close to $\propto N_p^{2/3}$, respectively) are those corresponding to the quasi-static approximation. However, it is very important to understand that these are a result of several coincidences and have no underlying physical meaning—the quasistatic broadening regime is never realized in the central part of the Lyman-α shape.

In one of the first experimental studies [16] in which the dependence of line broadening on the perturber mass was observed, it was noted that the width of the Balmer-α line scales as $1/\sqrt{M_p^*}$ and a more general $\propto\sqrt{T/M_p^*}$ dependence was suggested (one should recall that this was done prior to the publication of theoretical works introducing the ion dynamics effect, when the state-of-the-art models predicted very weak, if any, influence of ion motion). The $\propto 1/\sqrt{M_p^*}$ scaling was later confirmed by CSs of Balmer-α [17]. As was noted in [16], the $\sqrt{T}$ dependence could not be checked due to a limited range of temperatures attainable using their experimental setup. However, as we have shown using the TCP model, the temperature dependences of ions and electrons significantly cancel each other. Thus, based on the present discussion, we can state that such a measurement would have given a negative result—unless a way was found to vary ion temperature independently of T_e [18].

3.2. Non-ideal plasmas

Let us now discuss the applicability of the present model, assuming an ideal plasma, to realistic plasmas. First, the statement that impact broadening scales as $\propto N_p/\sqrt{T}$ is a certain over-simplification. There is an additional weak logarithmic dependence on N_p and T due to the cutoffs of the impact integral [9]; the upper one is usually taken to be the Debye screening length, but may need to be further modified [19], especially in very weakly coupled plasmas. This logarithmic correction can be included in the present model by assuming a respective weak dependence of parameter $\bar{\alpha}$ in equation (17) (which otherwise is a constant) on the upper impact cutoff.

There is also another closely related issue: since the results presented in this study assume an ideal plasma, while the number of particles in the CSs is finite, questions of validity of such an approach and associated uncertainties are obviously raised. Indeed, it can be shown [20] that, for example, the Lyman-α broadening due to a 10^{17}-cm^{-3}, 100-eV electron plasma simulated with 8000 perturbers underestimates the true width by as much as ~50%. For a realistic TCP, however, this may be a minor correction, since electron broadening is smaller by almost two orders of magnitude than the ion one for the same temperature and density (see figure 6). For a lower T, the relative contribution of electrons increases, but this logarithmic correction decreases; so, for example, for the entire plot of figure 6 the respective error never exceeds 10% (which is of the same order as the accuracy of the model). It is only for very hot/low density plasmas, where the ions are in the impact regime, that such a correction becomes important and needs to be included.

Finally, plasma correlation effects result in modifications of the ideal plasma microfield statistical properties [10]. These effects can be incorporated by introducing respective correction factors in the expressions of $w_{\rm dyn}$ and $w_{\rm qs}$ as was suggested in [14], resulting in appropriate corrections to $\bar{\alpha}$ and $\bar{\beta}$ in equation (17). It should be noted, however, that while high-n transitions (the focus of [14]) for which the ion broadening is often in the quasistatic regime, $\Delta n = 1$ transitions, and especially Lyman-α, are affected by this regime only in a rather narrow range of plasma parameters between the impact and rotational regimes. As a result, at least for up to moderately coupled plasmas, inaccuracies introduced by neglecting these corrections are likely to be minor. Indeed, this can be seen by comparing our ideal plasma results with CSs of Stark broadening in realistic plasmas [15], shown in figures 6 and 7. Although the expected tendency is clear, i.e. for lower temperatures (figure 6) or higher densities (figure 7) accurate calculations give smaller broadening values, the differences are on the order of only 10% for the plasma parameters considered.

4. Discussion

4.1. Frequency fluctuation model and rotational limit

According to the modern formulation [21, 22] of the frequency fluctuation model (FFM) [23], the lineshape is calculated as

$$L(\omega) = \frac{1}{\pi}\Re\frac{J(\nu;\,\omega)}{1 - \nu\, J(\nu;\,\omega)}, \tag{21}$$

where

$$\nu = C_0\, w_{\rm dyn} \tag{22}$$

and

$$J(\nu;\,\omega) \equiv \int \frac{L_{\rm qs}(\omega')\mathrm{d}\omega'}{\nu + \mathrm{i}(\omega - \omega')}. \tag{23}$$

Here, $L_{\rm qs}(\omega)$ is the area-normalized quasistatic profile and C_0 is an empirical constant. In the case of Lyman-α perturbed by the 'rotational' field (equation (1)),

$$L_{\rm qs}(\omega) = \frac{2}{3}\delta(\omega) + \frac{1}{6}\delta(|\omega| - w_{\rm st}) \tag{24}$$

and, therefore,

$$J(\nu;\,\omega) = \frac{2}{3(\nu + \mathrm{i}\omega)} + \frac{1}{6\left[\nu + \mathrm{i}(|\omega| - w_{\rm st})\right]}. \tag{25}$$

One can readily see that in the rotational limit ($\nu \ll w_{\rm st}$), the contribution of the second term in equation (25) to the line

centre ($\omega \ll w_{\rm st}$) is negligible. Therefore,

$$L(\omega) \approx \frac{2}{3}\frac{\nu}{3\pi}\frac{1}{(\nu/3)^2 + \omega^2}, \tag{26}$$

i.e. a Lorentzian with FWHM of $\frac{2}{3}\nu$. Evidently, using the full field instead of the rotational one, the same result (equation (26)) is obtained following similar arguments.

Thus, FFM correctly reproduces two features of the rotational broadening regime: the width of Lyman-α is only proportional to $w_{\rm dyn}$, i.e. it is independent of the microfield magnitude; and the core lineshape is Lorentzian. However *quantitatively*, the result is incorrect. For example, equating the $R \to \infty$ limit from figure 5 to $\frac{2}{3}\nu$, one obtains $\nu \approx 1.9 w_{\rm dyn}$, i.e. almost four times larger than $\nu = 0.5\ w_{\rm dyn}$ that provides the best results in the intermediate ion dynamics regimes both for low-n [24] and high-n [25] transitions. Practically the same conclusions were drawn from studying Lyman-α of hydrogen-like helium [8]: assuming either full or rotational perturbation fields, for conditions when $\nu \ll w_{\rm st}$ ($N_p = 10^{19}\,{\rm cm}^{-3}$, $T = 1$ eV) the FFM widths are 3–3.5 times smaller than those given by a few independent CS calculations. Furthermore, the FFM $R \to \infty$ width *does* depend on the atomic properties; namely, on the contribution $f_{\rm c.c.}$ of the central component relative to the total line intensity (for a Lyman-n transition, $f_{\rm c.c.} = n/(n^2-1)$ [14]). Indeed, a straightforward generalization of equations (24)–(26) to an arbitrary hydrogen-like transition with an unshifted central component gives $w_{\rm ffm} = {\rm f_{c.c.}}\nu$, contrary to a fixed value evident from figure 5.

4.2. Rotational broadening and microfield statistical properties

We note that a fixed (i.e. independent from the atomic properties of the radiator) broadening in the rotational regime can be understood recalling that rotation of the electric field with an angular frequency Ω results in splitting of the central component of the transition into three sub-components, shifted by $\ell\ \Omega$ [26], where $\ell = 0, \pm 1$ (for the specific case of Lyman-α, see [27]). Evidently, the typical plasma microfield rotation frequency, and its standard deviation can only be proportional to $w_{\rm dyn}$. It must be acknowledged, however, that these considerations explain neither the specific proportionality coefficient nor the Lorentzian shape of the broadening in the rotational regime. In addition, we note that a plain rotation leaves the central ($\ell = 0$) subcomponent unshifted; thus, even after averaging over a distribution of angular frequencies, this component will remain a δ-function. Even more generally, the same can be said about any two-dimensional (2D) trajectory of the electric field vector. Indeed, as long as $\vec{F}$ lies, for example, in the xy-plane, the $|2p0\rangle$ state remains unaffected by it, and therefore the $1s - 2p0$ transition component remains not broadened. Since motion in a central field is always 2D, an interesting corollary is that a single binary collision is unable to truly broaden the Lyman-α line.

As the lowest T data in figure 6 show, the assumption of independent w_i and w_e contributions implied by equation (20) should be questioned when both electrons and ions are in the rotational regime, even within the ideal plasma approximation. Not only does the total linewidth, calculated by CSs, significantly deviate from the model-based value, but it also becomes notably (~50%) *smaller* than the broadening due to electrons alone. This result, which might seem paradoxical at first, has a simple explanation. Indeed, as shown in [5], for an arbitrary distribution of charges $\{Z\}$ and velocities $\{v\}$ with total particle density N, a 'mean life' of field F is a certain function of F, expressed in units of

$$t_0 = \frac{N^{-1/3}}{30^{1/6}\pi^{1/2}}\left(\frac{\left\langle |Z|^{3/2}\right\rangle^{1/3}}{\left\langle |Z|^{1/2}v^2\right\rangle}\right)^{1/2}, \tag{27}$$

where the angular brackets denote an ensemble average. For a quasineutral TCP consisting of electrons and ions with charge Z_i and density $N_i = N_e/Z_i$, and neglecting the ion velocities compared to the electron ones, one obtains

$$t_0 \approx \left(1 + \sqrt{Z_i}\right)^{1/6} t_0^{(e)}. \tag{28}$$

In other words, the total field, formed by slower ions and faster electrons, changes on average not as fast as the field due to electrons alone. Since evidently $w_{\rm dyn} \propto t_0^{-1}$, it follows that if both electrons and ions are in the rotational regime, the total broadening is *smaller* than the electron broadening. While these considerations qualitatively explain the numerical results, the quantitative agreement is poor: for the hydrogenic TCP ($Z_i = 1$), equation (28) predicts the total width to only be $2^{1/6} \approx 1.12$ times smaller than the electron-caused rotational broadening. One reason for this discrepancy is that equation (27) describes the mean life of the field *magnitude*, whereas it is the field *direction* that is responsible for rotational broadening; an equivalent of equation (27) for the plasma microfield direction remains to be derived.

We hope that these open questions will stimulate future studies of plasma Stark broadening of the simplest atomic transition.

5. Conclusions

Spectral lines with a central, unshifted Stark component are broadened by plasma microfields in a unique manner, which manifests itself most unambiguously when broadening by a one-component plasma is considered. In particular, the quasistatic broadening regime is never realized for the lineshape core: instead, broadening changes from the impact regime to another, also dynamical in nature, 'rotational' broadening regime. In the latter, the linewidth only depends on the typical frequency of the plasma microfields (i.e. $\propto N_p^{1/3}(T/M_p^*)^{1/2}$) and is *independent* of both the microfield magnitudes and the atomic properties of the transition. These effects are most pronounced in the case of the Lyman-α transition of hydrogen or hydrogen-like ions. We found a simple analytic expression for the linewidth that models its change from the impact regime to the rotational one and is applicable to broadening of Lyman-α due to electrons and ions alike. The treatment is further extended to realistic two-component plasmas. Good

accuracy over a very large range of plasma parameters is verified by comparison to results from computer simulations.

For laboratory plasma conditions often found in experimental and theoretical studies of hydrogen Lyman-α ($N_e \sim 10^{17}$ cm^{-3} and $T \sim 1$ eV) it coincidentally happens that Stark broadening by electrons and ions is comparable by magnitude, yet due to their radically different masses is in regimes rather close to the impact and rotational limits, respectively. As a result, the total Lyman-α width has temperature and density dependences which *appear* to correspond to those of the quasistatic approximation, i.e. nearly constant and $\propto N_e^{2/3}$, respectively. However, we stress that this has no real physical meaning—the quasistatic broadening regime is never realized in the central part of the plasma-broadened Lyman-α Stark profile.

Acknowledgments

We are indebted to M Á González and Y Maron for critically reading the manuscript and helpful discussions. The work of ES was supported in part by the Israel Science Foundation.

References

[1] Griem H R 1997 *Principles of Plasma Spectroscopy* (Cambridge: Cambridge University Press)
[2] Dufty J, Konjević N, Lisitsa V and Stamm R 2008 A roundtable on the first 50 years of quantum theories of Stark broadening *SPECTRAL LINE SHAPES: Volume 15 XIX International Conference on Spectral Line Shapes Valladolid (Spain)* ed M A Gigosos and M Á González vol 1058 pp 373–9
[3] Gigosos M A 2014 Stark broadening models for plasma diagnostics *J. Phys. D: Appl. Phys.* **47** 343001
[4] Holtsmark J 1919 Über die Verbreiterung von Spektrallinien *Ann. Phys. (Leipzig)* **58** 577–630
[5] Chandrasekhar S and von Neumann J 1942 The statistics of the gravitational field arising from a random distribution of stars. I. The speed of fluctuations *Astrophys. J.* **95** 489
[6] Demura A V and Stambulchik E 2014 Spectral-kinetic coupling and effect of microfield rotation on Stark broadening in plasmas *Atoms* **2** 334–56
[7] Demura A V, Lisitsa V S and Sholin G V 1977 Effect of reduced mass in Stark broadening of hydrogen lines *Sov. Phys. J. Exp. Theor. Phys.* **46** 209–15
[8] Calisti A, Demura A, Gigosos M A, González-Herrero D, Iglesias C A, Lisitsa V S and Stambulchik E 2014 Influence of microfield directionality on line shapes *Atoms* **2** 259–76
[9] Griem H R 1974 *Spectral Line Broadening by Plasmas* (New York: Academic)
[10] Demura A V 2010 Physical models of plasma microfield *Int. J. Spectr.* **2010** 671073
[11] Bethe H A and Salpeter E E 1977 *Quantum Mechanics of One- and Two-Electron Atoms* (New York: Plenum)
[12] Stambulchik E and Maron Y 2010 Plasma line broadening and computer simulations: a mini-review *High Energy Density Phys.* **6** 9–14
[13] Stambulchik E and Maron Y 2006 A study of ion-dynamics and correlation effects for spectral line broadening in plasma: K-shell lines *J. Quant. Spectr. Rad. Transfer* **99** 730–49
[14] Stambulchik E and Maron Y 2008 Stark effect of high-n hydrogen-like transitions: quasi-contiguous approximation *J. Phys. B: At. Mol. Opt. Phys.* **41** 095703
[15] Gigosos M A and Cardeñoso V 1996 New plasma diagnosis tables of hydrogen Stark broadening including ion dynamics *J. Phys. B: At. Mol. Opt. Phys.* **29** 4795–838
[16] Wiese W L, Kelleher D E and Helbig V 1975 Variations in Balmer-line Stark profiles with atom-ion reduced mass *Phys. Rev.* A **11** 1854–64
[17] Gigosos M A and Cardeñoso V 1987 Study of the effects of ion dynamics on Stark profiles of Balmer-α and -β lines using simulation techniques *J. Phys. B: At. Mol. Opt. Phys.* **20** 6005–19
[18] Gigosos M A, González M Á and Cardeñoso V 2003 Computer simulated Balmer-alpha, -beta and -gamma Stark line profiles for non-equilibrium plasmas diagnostics *Spectrochim. Acta Part* B **58** 1489–504
[19] Rosato J, Capes H and Stamm R 2012 Influence of correlated collisions on Stark-broadened lines in plasmas *Phys. Rev.* E **86** 046407
[20] Rosato J, Capes H and Stamm R 2014 Ideal Coulomb plasma approximation in line shape models: Problematic issues *Atoms* **2** 253–8
[21] Calisti A, Mossé C, Ferri S, Talin B, Rosmej F, Bureyeva L A and Lisitsa V S 2010 Dynamic Stark broadening as the Dicke narrowing effect *Phys. Rev.* E **81** 016406
[22] Bureeva L A, Kadomtsev M B, Levashova M G, Lisitsa V S, Calisti A, Talin B and Rosmej F 2010 Equivalence of the method of the kinetic equation and the fluctuating-frequency method in the theory of the broadening of spectral lines *JETP Letter* **90** 647–50
[23] Talin B, Calisti A, Godbert L, Stamm R, Lee R W and Klein L 1995 Frequency-fluctuation model for line-shape calculations in plasma spectroscopy *Phys. Rev.* A **51** 1918–28
[24] Ferri S *et al* 2014 Ion dynamics effect on Stark broadened line shapes: A cross comparison of various models *Atoms* **2** 299–318
[25] Stambulchik E and Maron Y 2013 Quasicontiguous frequency-fluctuation model for calculation of hydrogen and hydrogenlike Stark-broadened line shapes in plasmas *Phys. Rev.* E **87** 053108
[26] Lisitsa V S 1994 *Atoms in Plasmas Springer Series on Atoms +Plasmas* vol 14 (Berlin: Springer)
[27] Ishimura T 1967 Stark effect of the Lymann alpha line by a rotating electric field *J. Phys. Soc. Jpn* **23** 422–9